Dynamic Confinement Effects in Polymer Blends. A Quasielastic Neutron Scattering Study of the Slow Component in the Blend Poly(vinyl acetate)/Poly(ethylene oxide)

M. Tyagi,[†] A. Arbe,*[,‡] A. Alegría,[‡,§] J. Colmenero,[†,‡,§] and B. Frick[||]

Donostia International Physics Center, Paseo Manuel de Lardizabal 4, 20018 San Sebastián, Spain, Centro de Física de Materiales (CSIC−UPV/EHU), Apartado 1072, 20080 San Sebastián, Spain, Departamento de Física de Materiales UPV/EHU, Apartado 1072, 20080 San Sebastián, Spain, and Institut Laue−Langevin, BP 156, 38042 Grenoble Cedex 9, France

Received March 5, 2007; Revised Manuscript Received April 14, 2007

ABSTRACT: Motivated by the observation of confinement effects for the poly(ethylene oxide) (PEO) component in the dynamically asymmetric blend with poly(vinyl acetate) (PVAc), 80% PVAc/20% PEO (*Macromolecules*, 2006, **39**, 3007), we have investigated the dynamics of the PVAc component in this blend. Quasielastic neutron scattering techniques—in particular, backscattering—have allowed selectively studying the self-motions of PVAc hydrogens in a mixture with deuterated PEO. Moreover, we have extended the temperature/frequency range investigated with complementary broad-band dielectric spectroscopy experiments. The influence of blending on the dynamical behavior of PVAc (the component with higher value of the glass transition temperature T_g) in the α-relaxation regime can be explained by the Lodge and McLeish model based on the concept of self-concentration. This means, the high-T_g component behaves in a "standard" way upon blending, contrary to the low-T_g diluted component PEO. We find that the crossover temperature T_c where the dynamics of PEO changes qualitatively from glass-forming polymer-like ($T > T_c$) to confined ($T \leq T_c$), coincides with the merging temperature of the α- and β-processes of PVAc in the blend, T_M. This provides a framework to explain the origin of the confinement for the low-T_g component in this blend. Above T_M, the diffusive motions involved in the structural relaxation of PVAc constitute the overwhelming dynamics. In such a mobile environment, PEO segments are able to fully relax at different length scales. Below T_M, the time scales in which the sublinear regime of the α-process develops become slower than the local β-process. Therefore, PEO chains find a surrounding local mobility which facilitates their own motions at short length scales, but the intermolecular correlations do not decay fast enough to accommodate PEO's large length scale dynamics.

I. Introduction

The question of the dynamical miscibility in thermodynamically miscible polymer blends is nowadays one of the hottest topics in polymer physics (see, for instance, the literature[1−9] and references therein). Interestingly, it has been found that segmental dynamics are strongly influenced by the presence of other chains, though two different mean relaxation times are usually still observed. Each time scale corresponds to the dynamics of each of the components modified by blending. This "dynamic immiscibility" that is observed is called "dynamic heterogeneity" , and by now it is commonly accepted to be a consequence of chain connectivity on the local effective concentration of polymer blends (the so-called self-concentration effect).[1,10]

In systems where components display very different glass transition temperatures T_g (extremely asymmetric blends from a dynamical point of view), the dynamic heterogeneity is magnified. This is the case of, e.g., poly(vinyl methyl ether)/polystyrene (PVME/PS) ($T_g^{PS} - T_g^{PVME} = 123$ K)[11−14] or poly(ethylene oxide)/poly(methyl methacrylate) (PEO/PMMA) ($T_g^{PMMA} - T_g^{PEO} \approx 200$ K).[15−22] Due to miscibility and PEO-crystallization problems, the study of the last system is restricted to compositions with less than 30% PEO. It was in these diluted PEO/PMMA blends where NMR studies[18,20] revealed clear deviations from the expected behavior (for instance, predictions in terms of the Lodge and McLeish model[1]) toward the average T_g of the blend, T_g^{blend}. The surprising observation of a decoupling of 12 orders of magnitude in the time scales of the two components brought evidence of a new emerging phenomenon under conditions of extreme dynamical asymmetry and dilution of the low-T_g component.

The concept of confinement induced by dynamic asymmetry in polymer blends was first invoked in dielectric spectroscopy studies.[14,23] For PVME blended with PS with concentrations of PS higher than 50% by weight, a confinement length of about 10 Å was suggested. The idea behind the dynamic confinement is that, approaching the average glass transition of the blend, the chain segments of the high-T_g component could be considered as static on the time scale of the segmental motions of the low-T_g component and the dynamics of the latter would correspond to the motional processes of mobile chains embedded within a more or less frozen environment formed by the high-T_g component. Hints of this phenomenon in the same system can also be identified in the work by Urakawa et al.[24] Later, by combining neutron scattering measurements and molecular dynamics (MD) simulations in PEO/PMMA, Genix et al.[21] also showed evidence of confinement signatures for PEO dynamics, as well as other dynamic anomalies as, for instance, almost logarithmic decay of the intermediate scattering function. Similar behavior was also found in a recent molecular dynamics simulation of a simple bead−spring polymer blend model.[25] In this case the anomalous behavior was interpreted in terms of high-order mode coupling theory transitions.

[†] Donostia International Physics Center.
[‡] Centro de Física de Materiales (CSIC−UPV/EHU).
[§] Departamento de Física de Materiales UPV/EHU.
[||] Institut Laue-Langevin.

10.1021/ma070539i CCC: $37.00
Published on Web 05/26/2007

To check the universality of the dynamic confinement phenomenon, in a previous work[26] we have selectively studied the dynamics of the PEO component in a blend with poly(vinyl acetate) (PVAc) ($T_g^{PVAc} = 314$ K, $T_g^{PEO} \approx 221$ K) with 80% PVAc in weight. This was carried out by means of quasielastic neutron scattering (QENS) on a sample where the PVAc component was fully deuterated. In this way, the scattered intensity is mainly dominated by the incoherent scattering from the hydrogens in PEO, revealing thereby the self-motions of this fast component. The results clearly showed the existence of a crossover temperature T_c for PEO dynamics at about 70 K above the calorimetric glass transition of the blend. Whereas above T_c the dynamical behavior of PEO can be considered as the "standard" for a supercooled polymer, clear signatures of confined dynamics were revealed below T_c. These findings were again interpreted as consequence of the freezing of the high-T_g component mobility when approaching its own T_g in the blend.

We want to emphasize that for the slow component there is not any reason, in principle, to expect a qualitatively different effect of blending in this kind of mixture than that observed for other high-T_g components in blends with weaker dynamic asymmetry. On the other hand, it is clear that PEO behavior should be dictated to a large extent by the matrix mobility. Therefore, the characterization of the dynamics of the slow majority component is of utmost importance to understand the mechanism of dynamic confinement in these asymmetric blends. This is just the objective of the present study: to determine how PVAc moves in the presence of PEO and try to relate the crossover in PEO dynamical behavior with some dynamical feature of PVAc in the blend.

Exploiting again the advantages of QENS (space-time resolution at molecular level and selectivity through isotopic substitution), we have now investigated the self-motions of PVAc hydrogens in the blend. The backscattering technique employed allows exploring length scales of the order of the typical interchain distances and below and accesses time scales in the mesoscopic region. We have mainly focused on the temperature region above the average glass transition of the blend, in the neighborhood of T_c and above, where PVAc dynamics is well centered in the dynamical window of the spectrometer. In order to extend this study toward lower frequencies, we have complemented the QENS measurements with broad-band dielectric spectroscopy (DS) experiments.

After the description of the samples and experimental techniques used in this work, we present the QENS results and the analysis method employed. In addition to the study in the supercooled liquid region, we show QENS data in the glassy state—below the average glass transition of the blend—to address also the influence of blending on the methyl group dynamics of PVAc. The discussion section briefly deals first with this subject, and then is focused on the characterization of PVAc dynamics in the blend above T_g^{blend}. The questions how it differs from that in the homopolymer and whether the Lodge and McLeish model is applicable to this component are answered with the combined QENS and DS results at hand. Finally, we discuss the possible mechanism for confinement of PEO.

II. Experimental Section

A. Samples. The sample investigated is the blend of protonated poly(vinyl acetate) (hPVAc) and deuterated poly(ethylene oxide) (dPEO) in 80/20 weight ratio. The molecular weights M_w of the samples involved are $M_w^{hPVAc} = 217$ kg/mol and $M_w^{dPEO} = 30$ kg/mol. Polydispersity is close to 1.05 for dPEO, while hPVAc exhibits a broader distribution characterized by a higher polydispersity of 1.5. The blend samples were prepared simultaneously for the DS and QENS measurements. The two components were dissolved in common solvent benzene for 3 days followed by slow evaporation of casting solvent at room temperature. The samples were kept at 333 K in vacuum for 10 days to ensure complete evaporation of benzene. The glass transition temperatures of homopolymers and blend were measured by means of a DSC-Q1000 differential scanning calorimeter from TA Instruments and taken as the midpoint in an upward temperature scan at 10 K/min. The T_g of pure hPVAc was found to be around 314 K, while the semicrystalline PEO showed a glass transition at 221 K. For the blend sample, a broad glass transition which is considered a feature of miscible blend was observed and an average T_g^{blend} of 280 K can be assigned according to the above definition.

B. Quasielastic Neutron Scattering. In a typical neutron scattering experiment, the measured intensity as a function of energy $\hbar\omega$ and momentum transfer $\hbar Q$ provides information on the dynamics and structure of the sample under investigation. The modulus of the momentum transfer Q is determined by the scattering angle θ and the wavelength of the incoming neutrons λ as $Q = 4\pi \sin(\theta/2)/\lambda$. The measured intensity contains incoherent and coherent contributions that are weighted according to the corresponding cross sections (σ_{inc}, σ_{coh}). The incoherent intensity reveals the incoherent scattering function, $S_{inc}(Q,\omega)$ which is related via Fourier transformations to the intermediate incoherent scattering function, $S_{inc}(Q,t)$ and with the self-part of the Van Hove correlation function, $G_s(r,t)$. In the classical limit, $G_s(r,t)$ is the probability of a given nucleus being at a distance r from the position where it was located at a time t before. Thus, incoherent scattering looks at correlations between the positions of the same nucleus at different times. On the other hand, coherent scattering deals with relative positions of atomic pairs and, hence, reveals structural features of the sample (see, as general references, refs 27−29).

1. IN16 Measurements. The QENS measurements were carried out on the hPVAc/dPEO sample at the Institute Laue-Langevin (ILL) in Grenoble. Working with a wavelength of 6.271 Å the IN16 backscattering spectrometer offers an energy resolution of nearly Gaussian shape and covers a Q range between 0.19 and 1.9 Å^{-1}. In the glassy state we performed short (about 1.5 h) QENS measurements at 2, 20, 30, 50, 100, and 150 K to characterize the PVAc methyl group dynamics in the blend. Above T_g^{blend}, QENS spectra were recorded between 360 and 440 K at an interval of 20 K during about 7 h. The sample was prepared inside the flat aluminum container as aluminum has a very low scattering cross section for neutrons. The sample thickness of 0.2 mm was chosen to provide a transmission higher than 90% allowing multiple scattering effects to be neglected. Because of the quasielastic contributions from methyl group tunneling,[30] it is not possible to determine the instrumental resolution function (completely elastic response) from measurements on this sample at low temperature. Therefore, the resolution function of the spectrometer $R(Q,\omega)$ was determined from the measurement of the inversely labeled sample dPVAc/hPEO[26] at 2 K, where tunneling is strongly suppressed by the isotopic effect[31] and the scattering is only elastic. The acquired data were corrected for detector efficiency, sample container and absorption using the standard programs available at ILL, thus finally providing the experimental scattering function $S_{exp}(Q,\omega)$. The neutron scattering cross sections for different atoms involved in the chemical formula of hPVAc and dPEO are as follows: $\sigma_{inc}^{H} = 79.7$ barn; $\sigma_{coh}^{H} = 1.76$ barn; $\sigma_{inc}^{D} = 2.00$ barn; $\sigma_{coh}^{D} = 5.59$ barn; $\sigma_{inc}^{C} = 0$; $\sigma_{coh}^{C} = 5.56$ barn; $\sigma_{inc}^{O} = 0$; $\sigma_{coh}^{O} = 4.23$ barn. Therefore, the intensity scattered by the blend sample is dominated by the scattering from hydrogens present in hPVAc and, thereby, provides information about the self-motion of such atoms, $S_{inc}^{H(PVAc)}(Q,\omega)$.

C. Dielectric Spectroscopy. This technique is sensitive to the dipolar fluctuations in the sample. Dielectric measurements were performed in a wide frequency range of 10 mHz to 1.8 GHz using two different experimental setups: In the range 10^{-2}−10^{7} Hz we used a high-resolution Alpha dielectric analyzer supplied by

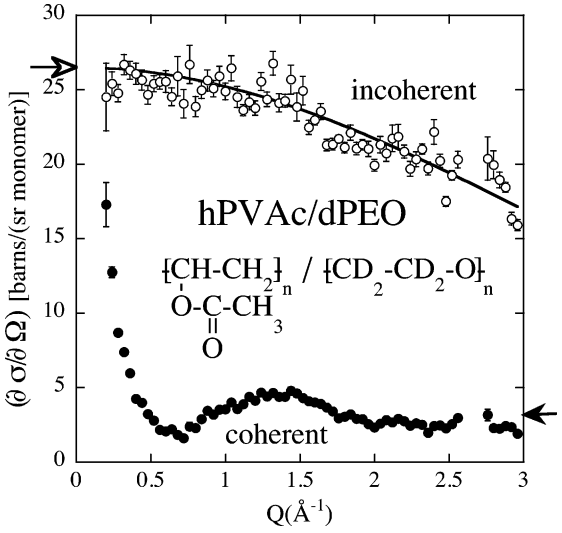

Figure 1. Coherent (full symbols) and incoherent (empty symbols) scattering cross sections obtained by D7 for hPVAc/dPEO at 400 K. The arrows indicate the theoretical values of $\sigma_{inc}/4\pi$ and $\sigma_{coh}/4\pi$. The solid line is a phenomenological description of the measured incoherent intensity in terms of a Debye−Waller factor-like expression.

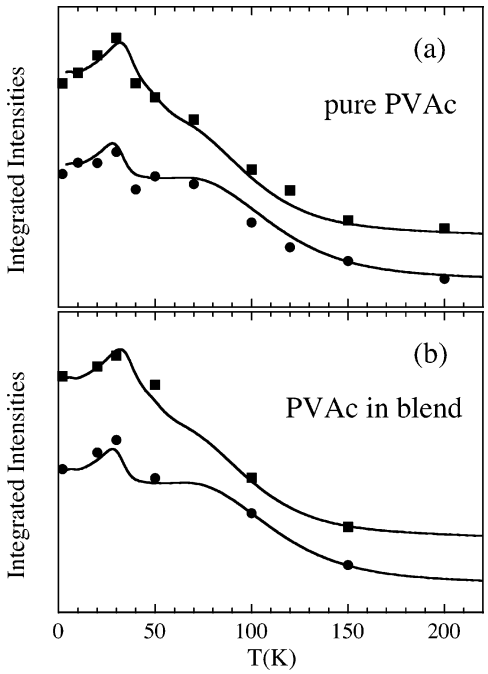

Figure 2. Experimental integrated inelastic intensities for PVAc[36] (a) and hPVAc/dPEO (b) at $Q = 1.8$ Å^{-1} in the intervals 1−2.5 (squares) and 2.5−6 μeV (dots). Solid lines correspond to the theoretical description by the general version of the RRDM with the parameters obtained for pure PVAc.[36]

Novocontrol GmbH and the range 10^6-10^9 Hz was covered with an Agilent impedance analyzer HP4291B. For both setups, samples were prepared between two gold plated electrodes of 30 and 10 mm diameters, respectively. Teflon spacers of 0.1 mm thickness and negligible area were used to maintain the constant distance between the two electrodes. Isothermal frequency measurements were carried out with a temperature stability better than 0.05 K. Further details about the setup, related accuracies, and calibration of the instruments can be found elsewhere.[32]

III. Results And Data Analysis

1. Contributions to the Scattered Intensity. Polarization analysis allows separation of coherent and incoherent contributions to the total intensity.[27,28] Instruments like D7 at the ILL offer this possibility. In our previous work on PEO dynamics in this blend,[26] we reported on D7 measurements on hPVAc/dPEO and dPVAc/hPEO. Here we recall that in the sample investigated in this work, hPVAc/dPEO, the D7 study confirms that the incoherent contribution is much stronger than the coherent one, as can be appreciated in Figure 1. These D7 results were corrected for multiple scattering effects using programs available at the ILL based on Monte Carlo simulation methods. The continuous decay of the incoherent cross section is due to inelasticity effects, which are extremely difficult to correct in samples with light nuclei.[33] However, we can see that in the low-Q limit (where such effects do not affect the signal) the incoherent data agree very well with the theoretically predicted value ($\sigma_{inc}/4\pi$), while at high-Q values the coherent contribution is very much compatible with the $Q \rightarrow \infty$ expected limit determined by $\sigma_{coh}/4\pi$. At sight of this figure, above $\approx$ 0.36 Å^{-1} the coherent contribution is less than 15% of the total intensity, and even in the very low Q range it remains much weaker than the incoherent signal. Taking into account that from the latter, more than 99% is due to PVAc hydrogens, we can safely consider the scattered intensity as completely determined by the self-motions of these atoms.

In ref 26, we also discussed in detail the effect of blending on the local structure on the basis of the coherent contributions isolated by D7 for the two samples. Summarizing, we showed that (i) the short-range order of PVAc chains is hardly affected by the presence of PEO (at least for the concentration investigated); (ii) experimentally it is impossible to isolate completely the structure factor of PEO in the blend, but for this component the results suggest larger and more distributed characteristic distances in the blend, or perhaps, less dense and stretched chains.

2. Methyl Group Dynamics in the Glassy State. Regarding methyl group rotations,[34] PVAc can be considered as a clear showcase. It was the first polymer—and indeed the first highly disordered system—where a complete investigation by neutron scattering was carried out on all the features of this dynamics (tunneling, crossover from quantum to classical hopping, hopping, and librations).[30,34−37] It was also the first system where a fully consistent description of the experimental results was achieved in terms of the rotation rate distribution model (RRDM).[34] This is shown in Figure 2a in a wide temperature range covering the tunneling as well as the classical regions and the crossover between them.[36] The RRDM assumes that the disorder in the glassy state leads to a distribution of potential barriers for this motion which in a first approximation can be taken as Gaussian. It is not the aim of this work to present in detail this model, but simply to show what is the influence of blending on methyl group rotations in PVAc. Figure 2b displays with symbols the corresponding experimental results on the blend. In this sample the relative incoherent contribution of the methyl group to the total scattering is slightly weaker than in pure PVAc (0.44 vs 0.46). This small correction has been taken into account in the calculation of the RRDM curves shown in Figure 2b, where we have assumed *just the same* distribution for the potential barriers used in pure PVAc. The fair reproduction of the blend experimental data by these functions evidence that the effect of blending on methyl group dynamics, if any, is really negligible.

3. Dynamics in the Supercooled Liquid Region ($T \gg T_g^{blend}$). Figure 3 shows the IN16 spectra obtained at $Q =$ 1 Å^{-1} and the different temperatures investigated. As described above, to a very good approximation they are entirely determined by the hydrogen motions in the PVAc component of the

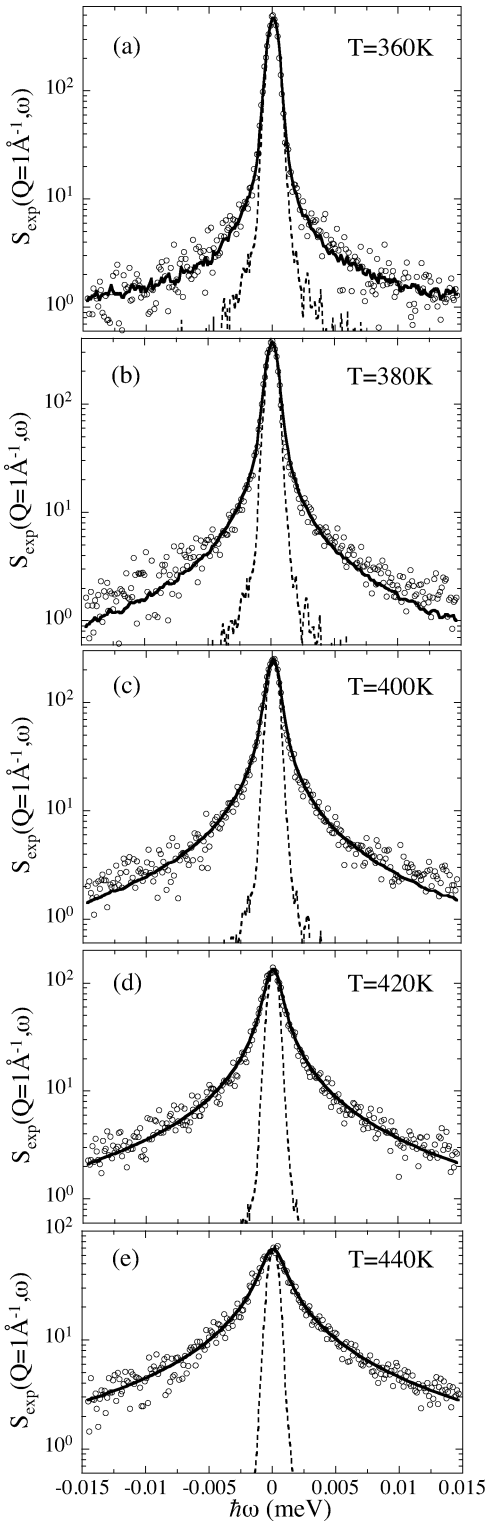

Figure 3. Spectra obtained by IN16 on the hPVAc/dPEO sample at $Q = 1$ Å^{-1} and different temperatures. The dotted line shows the resolution function (normalized to match the peak) and the solid lines are fits with KWW functions.

blend. A clear broadening with respect to the resolution function can be observed in all cases, which increases with increasing temperature. Having in mind that the quasielastic broadening is related with the inverse of the characteristic time of the motion observed, this figure shows that the dynamics becomes faster as the temperature increases. An inspection of the Q dependence at a given temperature (see, e.g., $T = 400$ K in Figure 4) reveals that there is a strong dispersion of the characteristic time: the decrease of the associated time scale with increasing Q value

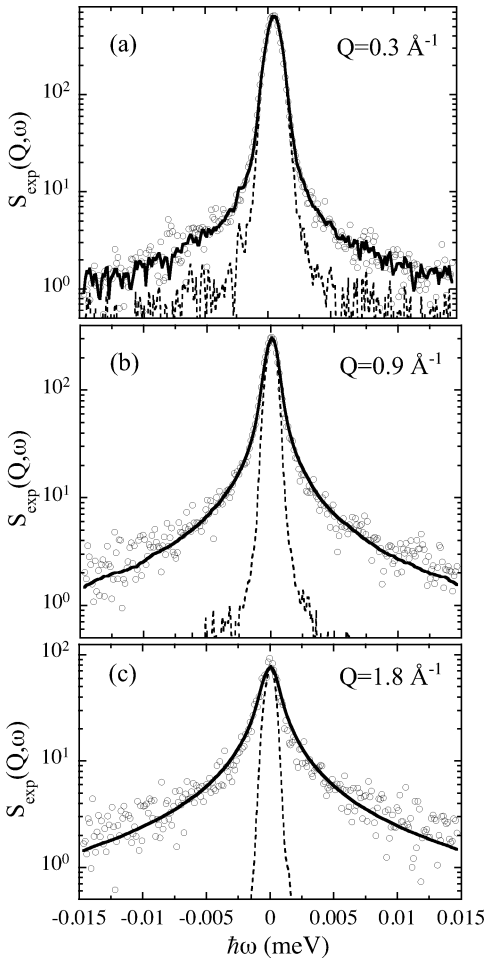

Figure 4. Spectra obtained by IN16 on the hPVAc/dPEO sample at 400 K and different Q values. Lines like in Figure 3.

reflects some kind of diffusive-like behavior in this temperature range well above the glass transition.

By now it is well-established that well above T_g, at local length scales—of the order of the intermolecular distances and below—and in the nanosecond region explored by, e.g., IN16, the main dynamical process driving the atomic motions in glass-forming systems is the decaging process involved in the structural or α-relaxation (see, e.g., ref 38). In such a range, the intermediate scattering function describing this phenomenon can be approximated by a stretched exponential or Kohlrausch−Williams−Watts functional form:

$$S^{KWW}(Q,t) = A(Q,T)\exp\left[-\left(\frac{t}{\tau_{KWW}}\right)^{\beta}\right] \qquad (1)$$

Here β is the stretching parameter describing the deviations from exponential behavior ($0 < \beta \leq 1$, and close to 0.5 for most polymers[39]) and τ_{KWW} the characteristic time which depends on Q and T. Equivalently, the Fourier transform of eq 1 describes the scattering function in the frequency domain. The prefactor $A(Q,T)$ determines the amplitude of the function.

In order to fit the experimental spectra, the theoretical function was convoluted with the resolution function of IN16, $R(Q,\omega)$:

$$S_{exp}(Q,\omega) = S^{KWW}(Q,\omega) \otimes R(Q,\omega) \qquad (2)$$

We note that in this way we implicitly neglect the effect of possible different dynamical behavior of contributions other than PVAc hydrogens—which is justified by their small influence

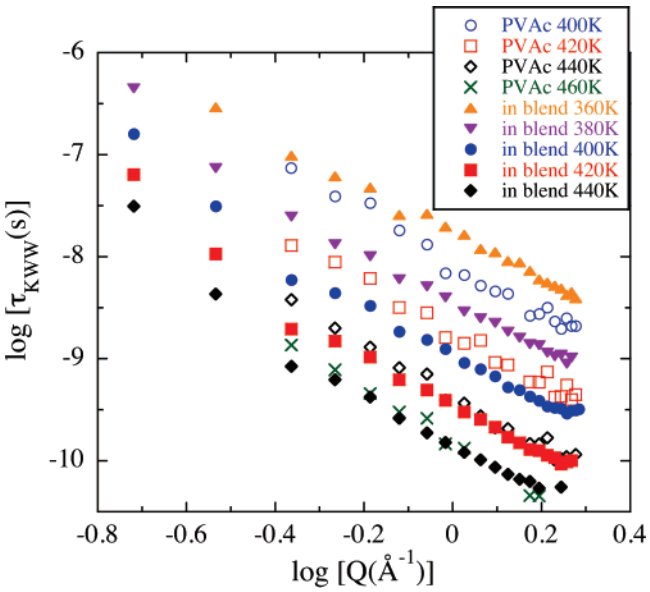

Figure 5. Momentum transfer dependence of the characteristic times obtained from the KWW fit to the IN16 spectra of hPVAc/dPEO at the different temperatures investigated (full symbols). For comparison, the times corresponding to pure PVAc[32] are also shown with empty symbols.

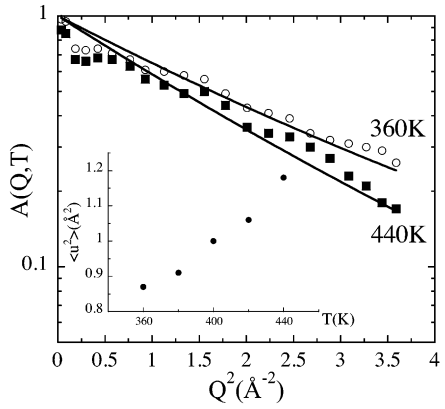

Figure 6. Momentum transfer dependence of the amplitudes $A(Q,T)$ obtained at 360 and 440 K. The solid lines correspond to fits to eq 4. The inset shows the such obtained values for the mean squared displacement associated with the fast processes.

in the spectra. Our approach also implies assuming identical parameters for all kinds of hydrogens in the sample. The fitting of QENS data was done using a nonlinear optimization program to minimize the squared difference between predicted and measured values. We first determined the value of the shape parameter β. At a given temperature, β was used as free parameter for a number of Q values to cover the entire Q range. For example, for the lowest temperature investigated we obtained $0.42 \leq \beta \leq 0.52$ and for the highest, $0.46 \leq \beta \leq 0.57$. Taking into account the uncertainties, and in view of the small dispersion of the average value around 0.5 ($\langle\beta\rangle_{360K} = 0.46$; $\langle\beta\rangle_{380K} = 0.49$; $\langle\beta\rangle_{400K} = 0.49$; $\langle\beta\rangle_{420K} = 0.52$; $\langle\beta\rangle_{440K} = 0.53$), we fixed the value of this parameter to 0.5 for the subsequent analysis at all temperatures. In Figures 3 and 4, the good agreement between the fitting curves and the experimental data can be appreciated. The such obtained Q- and T-dependent characteristic times are displayed in Figure 5 together with those reported for pure PVAc in ref 32. For the lowest and highest temperatures investigated, the values of the amplitudes are shown as a function of Q in Figure 6.

IV. Discussion

1. Methyl Group Dynamics. We have found that the dynamics of PVAc methyl groups in the glassy state is indistinguishable in the blend and in the homopolymer. The same conclusion was drawn for methyl group rotations in other blends: PVE/PS,[40] PEO/PMMA,[21] and head-to-head polypropylene (hhPP)/poly(ethylene propylene) (PEP)[41]. Thus, at least in systems exhibiting weak intermolecular coupling, blending does not appreciably affect fast motions and processes active in the glassy state. In fact, this has also been proven for the subpicosecond dynamics of hhPP/PEP[41] and for secondary relaxations (DS on PVME/PS,[13] PVME/poly(*o*-chlorostyrene) (PoClS)[42] and PEO/PMMA,[17] and QENS on polyisoprene (PI)/poly(vinyl ethylene) (PVE)[43]) (all these are blends with weakly interacting components). Such behavior is probably a consequence of the rather localized character of the motions involved in these processes.

2. Dynamics above the Glass Transition. We commence with the discussion of the amplitude $A(Q,T)$. $A(Q,T) < 1$ has its origin in the decay of the correlations at times faster than those accessible by the spectrometer. Such decay is produced by vibrational processes including the boson peak (see, e.g., ref 44) and other fast motions (like the so-called "fast dynamics" [see, e.g., refs 44 and 45]). Usually, it is assumed that the reduction in the amplitude due to the fast processes taking place in these systems can be approximated by a Debye−Waller factor-like expression involving the mean squared displacement of the atoms associated with the fast localized motion $\langle u^2\rangle$. In the case of PVAc, the fast methyl group rotations in this temperature range lead also to an additional reduction of the amplitude described by the elastic incoherent structure factor EISF of such motion, expressed by the following:[29]

$$\mathrm{EISF} = \frac{1}{3}\left[1 + 2\frac{\sin(Qr_{HH})}{Qr_{HH}}\right] \qquad (3)$$

Here r_{HH} is the distance between hydrogens in the methyl group. Under the (implicitly assumed) hypothesis that methyl group hydrogens simultaneously rotate and participate in the overall dynamics and considering as a first approximation the same value of $\langle u^2\rangle$ for all atoms in the system, the amplitude of the spectra can be described as

$$A(Q,T) = \exp\left(-\frac{\langle u^2\rangle Q^2}{3}\right)[f_{MG}EISF + (1 - f_{MG})] \qquad (4)$$

where f_{MG} is the relative fraction of incoherently scattered intensity due to methyl group hydrogens (0.44). Figure 6 shows that eq 4 can describe reasonably well the obtained amplitudes. The slight modulation of the data is related with the use of a resolution function measured on another sample, which makes difficult to correct the small coherent contributions. Nevertheless, a temperature dependent $\langle u^2\rangle$ can be obtained from this analysis which is shown in the inset of the figure. The values of this parameter lie well in the range observed usually for polymers in this temperature range (see, e.g., refs 41 and 46). A direct comparison with the values obtained for pure PVAc is difficult, since they are subject of a rather high uncertainty due to the limited Q value explored in that IN16 experiment.[32] They can be quoted between 0.8 and 1.1 Å^2 in the range 400−460 K, i.e., taking rather similar values to those observed in the blend. This implies that the fast processes, within the uncertainties, show approximately the same spatial extent in

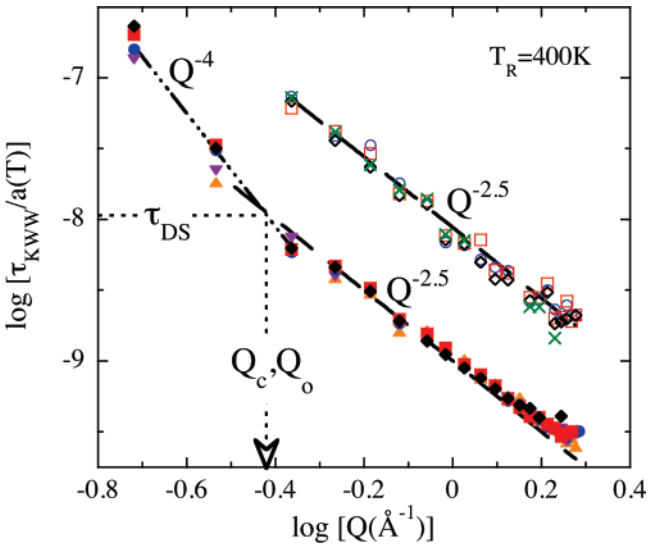

Figure 7. Master curves obtained for PVAc pure and in the blend with PEO with a reference temperature of 400 K. Symbols as in Figure 5. The dashed lines correspond to power-laws characterized by $\tau_M \propto Q^{-2.5}$, while the dashed-dotted line depicts $\tau_M \propto Q^{-4}$. For the blend data, the vertical arrow indicates the Q value where both power-laws intersect (Q_c), which coincides with the Q value for which the DS time scale (constant value shown by the dotted horizontal line) matches the IN16 results (Q_o).

the pure sample and in the blend, as could be expected for localized motions.

Contrary to local processes, the dynamics in the α-region of PVAc is clearly modified by the presence of PEO chains. As shown in Figure 5, for a given Q and T, the time scale in the blend is accelerated with respect to that in the homopolymer. This was expected on the basis of the vast literature on polymer blends, where this effect is unfailing reported for the α-relaxation of high-T_g component of the blend. On the other hand, within the uncertainties the values of the shape parameter β used in both cases are the same, i.e., the functional form of the intermediate scattering function is not appreciably influenced by blending, at least in the temperature range here investigated. This has also recently been observed in the same system from molecular dynamics simulations results.[47] In this range, this result is commonly found, since the role of the concentration fluctuations leading to an extra broadening of the signal[5,48−52] is not very important. Regarding the Q dependence of the characteristic times, in the Q range where data from both samples are available ($0.43 \leq Q \leq 1.9$Å^{-1}) the behavior seems to be very much the same in the homopolymer and in the blend.

In order to better determine the Q and T dependence of these times in both samples, we have constructed the master curves shown in Figure 7. Thereby, we have considered a reference temperature of $T_R = 400$ K and shifted the data corresponding to the different temperatures toward T_R. The resulting superposition is almost perfect, indicating that the Q dependence is nearly identical for all temperatures investigated. Power-laws ($\tau_M \propto Q^{-x}$) with the same exponent $x = 2.5$ can describe the two master curves for $Q \geq 0.43$ Å^{-1}. We note that this value of the exponent (2.5) is much lower than the value $2/\beta$ (4, in this case) corresponding to the Gaussian behavior[53] reported for a large number of polymers.[39] Recently, deviations from Gaussian approximation in the high Q range have also been observed in several polymers.[41,54−63] In those cases, a crossover toward the expected Gaussian regime is found at a crossover momentum transfer, Q_c, which is located within the IN16 window [Q_c values between about 0.65 and 1.3 Å^{-1}]. This crossover is indeed also found in our blend data, which extend up to 0.19 Å^{-1}. They show a clear change in slope at about $Q_c \approx 0.4$ Å^{-1}, reaching the Gaussian regime $\tau_M \propto Q^{-2/\beta}$ below Q_c. It is noteworthy that this is the lowest value reported until now for Q_c, indicating thus the largest deviations from Gaussian behavior at local scales. Unfortunately, the restricted Q range of the reported IN16 measurements of pure PVAc[32] prevented this observation. However, recent molecular dynamics simulations and neutron spin echo experiments on this system have allowed extending the Q range investigated toward low-Q values, evidencing finally also such a crossover.[64]

PVAc thus shows strong deviations from Gaussian behavior both, as homopolymer and also in the blend with PEO. The origin of this observation was discussed in ref 32 for pure PVAc, and was attributed to the possible existence of heterogeneities in the system even at such high temperatures. Heterogeneity inherent to the different dynamics associated with the diverse kind of hydrogens in the sample (side group vs main chain) was proposed to be—at least partially—the reason for the strong deviations from Gaussian behavior observed in PVE.[63] This kind of heterogeneity could indeed also play a significant role in this case. Finally, in the framework of an anomalous jump diffusion origin of the α-relaxation,[58,62] this behavior would be consequence of the distributed elementary jumps behind the subdiffusive atomic motions in the segmental relaxation. If this model holds, every system should show such deviations. However, at hand of the existing studies in the literature, which report elementary jump distances of the order of 0.5 Å, the crossover from Gaussian to non-Gaussian behavior should take place in the range $Q_c \approx 1$ Å^{-1}.[62] PVAc pure as well as in the blend displays the crossover at much lower Q values, suggesting additional sources for this kind of deviations as the heterogeinities above-mentioned, or perhaps a larger spatial extent of the elementary processes behind the decaging than those in other polymers (revealing themselves thus with a smaller Q_c).

As mentioned, in the overlapping Q range for both samples we did not find evidence for influence of blending on the Q dependence of the time scales. In other regular blends investigated by this technique and in similarly high-temperature regions, PI/PVE[43,65] and hhPP/PEP,[41] the effect of blending on the dispersion of the time scales—if any—was also negligible.

The information on the T dependence of the dynamics is contained in the shift factors $a(T)$ employed for building the master curves. However, to determine the effect of blending we have to compare the time scales corresponding to PVAc in the blend and in pure PVAc at the same Q value. We have chosen $Q = 1$ Å^{-1} as representative for the IN16 window. Starting from $\tau_M(Q = 1$ Å$^{-1})$ (the value deduced from the fitting power-laws to the master curves) we have defined the time scales $\tau_M(Q = 1$Å$^{-1})a(T)$ shown in Figure 8. This figure reveals a clear shift of the time scales in the blend toward lower temperatures. Does this shift correspond to the difference between the glass transition temperatures of pure PVAc and hPVAc/dPEO as determined by calorimetric measurements ($T_g^{PVAc} = 314$ K, $T_g^{blend} = 280$ K)? As can be seen in Figure 9a, such a shift, by 34 K, allows one to match the time scales in the low-T region; however, it does not work very well at high temperatures. The best agreement is achieved by applying a smaller shift in temperature of about 28.5 K (see Figure 9b). This suggests that the "effective" glass transition of the PVAc component in the blend does not occur exactly at the temperature deduced from DSC but is higher, i.e., shifted toward the homopolymer glass transition.

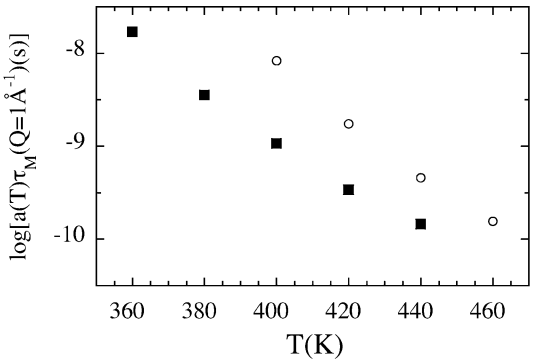

Figure 8. Temperature dependence of the shift factors used to build the master curves in Figure 7 (empty circles, pure PVAc; full squares, PVAc in the blend). They are multiplied by the value of the time deduced from the power law fitting the master curve (solid lines in Figure 7) at $Q = 1\text{Å}^{-1}$.

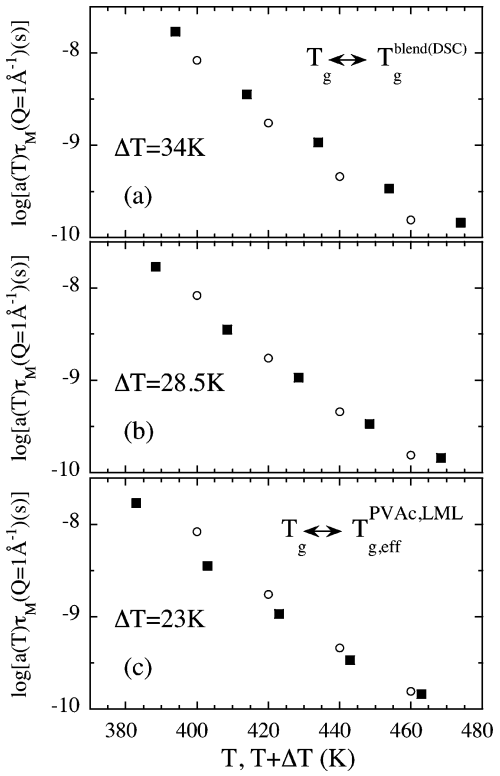

Figure 9. For pure PVAc (empty circles), the same representation of the time scales as in Figure 8. For the blend (full squares), the time scales from Figure 8 are displayed against $T + \Delta T$, with $\Delta T = 34$ (a), 28.5 (b), and 23 K (c).

This kind of behavior is indeed expected in the framework of the models based on the concept of self-concentration[1,10,66] trying to explain the dynamic heterogeneity in miscible polymer blends. The idea is that the local concentration around one segment of one of the blend components will be always richer in this component due to the chain connectivity. As the average glass transition in the blend depends on composition, both components experience different "effective glass transitions" $T_{g,eff}$. These different glass transitions, in fact, imply different relaxation times for both components. The most elaborated formulation of this kind of models is that proposed by Lodge and McLeish (LML),[1] who consider that the relevant length scale for segmental dynamics is of the order of the Kuhn length l_K. Then the self-concentration of the considered component ϕ_s in the relevant volume $V \sim {l_K}^3$ is calculated as

$$\phi_s = \frac{C_\infty M_0}{k\rho N_{av} {l_K}^3} \tag{5}$$

where M_0 is the molecular mass of the monomeric unit, k is the number of backbone bonds per repeat unit, N_{av} is the Avogadro's number and ρ is the density. For PVAc, the average backbone bond length l is close to 1.55 Å; considering the reported value of the characteristic ratio $C_\infty = 8.79$[67,68] a Kuhn length of $l_K \approx 13.6$ Å is deduced. Thus, for this polymer $\phi_s \approx 0.23$ can be estimated from eq 5. Another ingredient of this model is the hypothesis that, apart from the self-concentration, the composition of volume V around a given segment is the macroscopic one. In those conditions, there is no distribution of relaxation times involved and the model only deals with the mean relaxation time of each of the blend components. Applying these ideas to the case of PVAc in our blend, its "effective concentration"

$$\phi_{eff} = \phi_s + (1 - \phi_s)\phi \tag{6}$$

is 0.85 instead of $\phi = 0.80$. The "effective glass transition temperature" $T_{g,eff}^{PVAc,LML}$ (i. e., corresponding to the effective concentration) can be estimated from the concentration dependence of the average glass transition of the blend $T_g^{blend}(\phi)$. To avoid using, e.g., a simple Fox equation, we used experimentally determined values in the region of concentrations around 0.85. Considering the T_g values for pure PVAc ($T_g^{PVAc} = 314$ K), the blend studied here ($T_g^{blend}(\phi = 0.80) = 280$ K) and an additional blend of 90hPVAc/10dPEO ($T_g^{blend}(\phi = 0.90) = 300$ K), a smooth curve between the PVAc weight fractions 0.80 and 1 can be generated. According to this approach, we would estimate the value corresponding to 85% of PVAc to be 291 K. This is thus the value of $T_{g,eff}^{PVAc,LML}(\phi = 0.80)$.

We may check whether this predicted value of $T_{g,eff}^{PVAc,LML}$ reproduces PVAc behavior in the blend as observed by QENS in the IN16 window. This is done in Figure 9c. As we can see, this shift brings together well the high-temperature results, but seems to be inadequate at the lowest temperatures investigated.

We note that the temperature range explored by IN16 is too narrow and centered in too high temperatures to really determine univocally a T_g value for the PVAc component in the blend. For this reason we have complemented our study by DS measurements, which allow extending the temperature range and easily approaching the glass transition region. As shown in a recent work on this blend,[69] the DS signal reveals predominantly the dynamics of the PVAc component. The characteristic time scales (defined as the inverse of the maxima of the dielectric loss, τ_m) obtained for pure PVAc and the blend are depicted as a function of temperature in Figure 10. It is well-known that the usual thermal dependence of the time scale associated with the α-relaxation of low molecular weight glass formers and pure polymers can be well described using Vogel−Fulcher−Tamann (VFT) or Williams−Landel−Ferry (WLF) functions. These two formulations are equivalent from mathematical point of view. However, the presence of T_g in WLF equation makes it more suitable to predict the time scales for LML model by just shifting the T_g value. Therefore, we have fitted the relaxation times for pure PVAc to WLF equation:

$$\log \tau_m = \log \tau_m(T_g) - \frac{C_1(T - T_g)}{C_2 + (T - T_g)} \tag{7}$$

The two constants C_1 and C_2 are found to be 14.37 and 46.48 respectively. Now, in order to see the predictions of LML model,

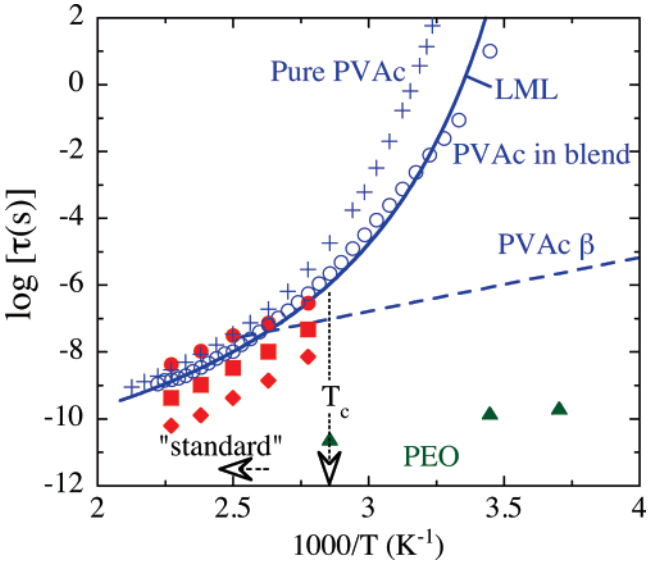

Figure 10. Temperature dependence of the time scales (inverse of the maximum frequency) obtained by DS for the α-relaxation of pure PVAc (pluses) and PVAc in the blend (empty circles). Solid line shows the prediction of LML model for PVAc component in the blend. Dashed line is an extrapolation of the relaxation time reported for the β-relaxation of PVAc.[70] The KWW-time scales obtained by QENS for PVAc in the blend are shown as full circles (0.3 Å^{-1}), squares (0.65 Å^{-1}) and diamonds (1.5 Å^{-1}), while the triangles correspond to the localized time observed for PEO in the blend ($Q \approx 1.5$ Å^{-1}). The vertical arrow marks the temperature (350 K) where the crossover in PEO dynamics occur in this blend, T_c. For 375 and 400 K, equilibrium dynamics is observed for this component.

we just have to replace the T_g value by $T_{g,eff}^{PVAc,LML} = 291$ K. As can be seen in Figure 10, the overall agreement between the DS experimental data for the blend and the such modified WLF equation is very good. Some deviations can be seen at lower temperatures. However, at these temperatures the uncertainty in time scales is higher because of conductivity/interface contributions from the hPVAc/dPEO blend sample. Therefore, we can say that, within experimental uncertainty, the prediction of the LML model is consistent with the observed effect of blending on the high-T_g component of the mixture.

Figure 10 also displays the time scales obtained for PVAc in the blend from IN16 at three different Q values. For comparison, we have also included the time scales of PEO in the blend at $Q \approx 1.5$ Å^{-1}. We can appreciate that PEO dynamics is much faster than that of PVAc. In fact, at 375 and 400 K—the highest temperatures investigated for the fast component in our previous work[26]—the PEO time scale is out of the IN16 window in the Q range above ≈ 1 Å^{-1}. This is thus a clear example of the dynamic heterogeneity in polymer blends. On the other hand, focusing again on the PVAc component, Figure 10 shows that the time scales of this component display nearly the same temperature dependence independently of the Q value considered. However, it can be seen that this dependence is weaker than that observed by DS for the segmental relaxation. In the figure we have also included the extrapolation of the characteristic time obtained by DS for the β-relaxation in PVAc.[70] After the above discussion, we may assume that this local process is not very much influenced by blending and thus the dashed line would also represent the PVAc secondary relaxation in the blend. As we can realize, at the lowest temperature investigated by QENS (360 K) the time scale of the β-process is just in the range of the time scales observed by IN16. This suggests that in this temperature range the atomic motions revealed by the neutron spectra reflect, in addition to the anomalous diffusion involved in the α-relaxation, the influence of the localized motions leading to the β-process. Pure PVAc neutron data would be less influenced by the β-process because the temperature range explored in that case is centered at higher temperatures (400−460 K). Thus, the deviations from scaling at low temperature in Figure 9c could be attributed to the influence of β-like processes in the blend data, which accelerate the observed time scale. In fact, we realize that in the high-temperature region where no influence of the β-process is expected, the value of $T_{g,eff}^{PVAc,LML}$ provided the right shift for the time scales in the blend to match those in the homopolymer (see Figure 9c). In this way, we can rationalize why the apparent $T_{g,eff}^{PVAc}$ is different for IN16 and DS results.

We can appreciate in Figure 10 that the values of the DS times of the blend are located between those obtained from IN16 at 0.3 and 0.65 Å^{-1}. Though the definition of the time scales is not exactly the same (KWW times for IN16 and τ_m for DS), these times are representative for the locations of the maxima of the associated (at least from a mathematical viewpoint) distribution function of relaxation times. Thereby, they can be considered as representative for direct comparison of the main characteristic time scales. At high-temperature—where the apparent activation energies are the same for both kinds of results—the Q value at which QENS delivers the same time scale as DS is $Q_o \approx 0.4$ Å^{-1} (see Figure 7). This Q value is slightly lower than that matching pure PVAc data ($Q_o \approx 0.65$ Å^{-1}),[32] which in fact was already significantly lower than most values reported for other polymers ($Q_o \approx 0.9-1.4$ Å^{-1}).[21,54,56] Those values were obtained from the comparison of NS (or MD simulations) results on the incoherent time for hydrogens with DS or NMR results (either experimental or obtained from MD-simulations) for several polymers. Up to date, hhPP is the only case where a similarly low Q_o value ($Q_o = 0.65$ Å^{-1}) has been reported to match NS and DS data.[41] The question that arises is whether Q_o could reveal some relevant length scale associated with the relaxation techniques. It is clear that both, DS and NMR techniques are probing relatively local length scales (DS through reorientations of the molecular dipoles, NMR through reorientations of bonds). Though a definite interpretation of the associated length scale to the matching Q value is not yet worked out, it was pointed out in refs[41,56] that Q_o usually lies in the region where the crossover from Gaussian to non-Gaussian behavior is observed in the incoherent scattering function (which we have called Q_c). In fact, we realize that this is again the case for PVAc in the blend (see Figure 7) and in the homopolymer, as reported in ref 64. Thus, our results strongly support that hypothesis, taking into account the unusual values of both, Q_c and Q_o found for PVAc. This seemingly general observation would lead to think that NMR and DS techniques would be somehow sensitive to the heterogeneities and non-Gaussian processes discussed above which cause the deviations from Gaussian behavior. Finally, we note the approximate coincidence of the value of Q_c and Q_o with the position of the first peak of the static structure factor of PVAc ($Q_{max} \approx 0.7$Å^{-1}).[26] This maximum is also observed at lower Q values than in many other polymers (e.g. $1.0 \leq Q_{max} \leq 1.5$Å^{-1} for 1,4- and 1,2-polybutadiene, polyisoprene, polyisobutylene, poly(vinyl chloride), and atactic polypropylene; see ref 39 and references therein).

3. Origin of Confinement Mechanism for PEO. Let us now discuss the general framework provided by the complementary studies of the two blend components (this work and ref 26) for the dynamics of the blend PVAc/PEO (80/20) above and around the average glass transition T_g^{blend}. In the previous discussion we have shown that the influence of PEO chains on PVAc

dynamics is accounted for by the model proposed by Lodge and McLeish, as it is the case of a large number of blend components [for instance, PS in different blends,[4,72] poly(ϵ-caprolactone) (PCL) in polycarbonate (PC),[73] or in blends of PVE and various polyethers[8]]. In other cases, this model also works, allowing a slight variation of ϕ_s (or the relevant length scale) with temperature [for example, for PVE in PVE/PI,[5] for PoCls in PoClS/PS,[74] for hhPP in hhPP/PIB[5]]. In general, we can say that by now the validity of the LML model is well established and provides semiquantitative predictions. This statement seems to hold also for the high-T_g component in this extremely dynamical asymmetric blend. However, this model happens to fail for the low-T_g component, PEO, in a certain temperature range. The following points summarize the main conclusions of our previous work on the PEO dynamics in this blend:[26]

•Close to T_g^{blend}, the incoherent scattering function of PEO hydrogens shows an extremely broad feature. Distributions of relaxation times extending over many decades have to be used to describe the spectra. The observation of Q-independent distributions at $Q \gtrsim 1.25$ Å^{-1} strongly suggests the localized character of the observed dynamics. The dramatic increase of the characteristic time toward lower Q values could be interpreted as due to the freezing of the large-scale motions for PEO chains.

•At high temperatures (375 and 400 K, i. e., $\approx T_g^{blend} + 100$ K) the PEO behavior is rather close to that expected for the low-T_g component of a regular miscible blend regarding both, the spectral shape and the dispersion of the characteristic times.

•It is around $T_c \approx 350$ K ($T_g^{blend} + 70$ K) where the crossover between both *qualitatively different* dynamical regimes takes place. This manifests itself through deviations from standard polymer melt dynamics below ≈ 0.7 Å^{-1} with respect to both, the spectral shape and the Q dependence of the average times.

In the present study on the PVAc component we have determined the mobility of the slow majority polymer in a wide temperature interval above and close to the crossover region ($T_c \approx 350$ K) where PEO dynamics changes qualitatively. As can be seen in Figure 10, T_c is located where the α and β-processes of PVAc (as determined by DS) merge. This suggests the following possible interpretation: only when PVAc segmental dynamics in the blend is similar or faster than the local motions involved in its secondary relaxation can PEO segmental dynamics develop without severe constraints in a mobile environment. At 375 and 400 K, PEO shows "standard" dynamics (that expected for a polymer melt). If we look at Figure 11, we realize that at 400 K the time scale extrapolated for the local motions of the PVAc β-process (lower horizontal line) lies in the region where the Gaussian regime corresponding to the sublinear diffusion in the α-relaxation is fully established. Thus, in this temperature range, the diffusive motions involved in the structural relaxation constitute the overwhelming dynamics. In such mobile environment, PEO segments are able to fully relax at different length scales. However, at 360 K (close to T_c) the time scales in which the sublinear regime of the α-process develops (at $Q \lesssim Q_c$) become slower than the local β-process (upper horizontal line in Figure 11). In fact, we have seen that the 360 K QENS results seem to be somehow influenced by this process. Therefore, PEO chains find a surrounding local mobility which facilitates their own motions at short length scales. However, at larger length scales the environment is rather stiff and only relaxes at longer times, leading to the freezing of large-scale dynamics also in PEO. With decreasing temperature, the situation is expected to become even more dramatic. PEO localized motions can develop toward lower temperatures thanks to the remaining mobility of the matrix due to the local motions of the PVAc secondary process; simultaneously, the α-relaxation of this component freezes and the intermolecular correlations do not decay fast enough to accommodate large length scale dynamics of PEO. Further work on other blend systems is necessary to check whether or not this interpretation is correct.

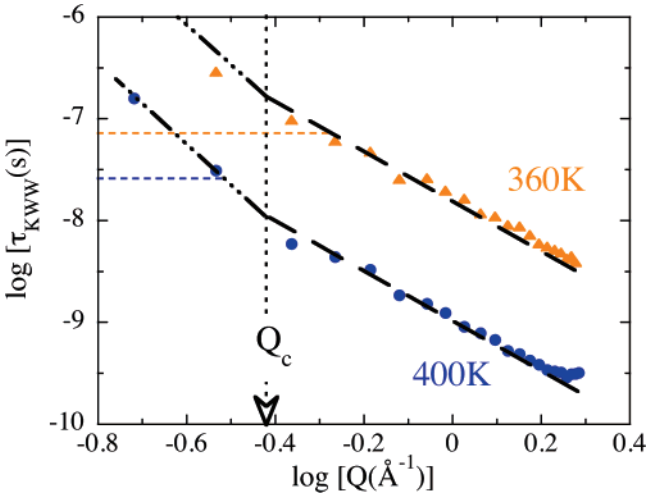

Figure 11. Comparison of the IN16 characteristic times for hPVAc/dPEO at 360 (triangles) and 400 K (circles) with the time scales extrapolated from DS for the β-process at the same temperatures (horizontal dotted lines). The meaning of the rest of the lines as in Figure 7.

Finally we mention recent SANS studies on the PS/PVME system,[75] which is also dynamically asymmetric and shows this kind of confinement effects for the PVME (low-T_g) component.[14] This investigation has shown anomalous behavior in a region between the two polymer glass transitions.[75] There, the blend behaves in a gel-like limit at which concentration fluctuations relax more quickly than rheological relaxation. These results have been interpreted within the theoretical framework of dynamical coupling between stress and diffusion.[76] In this direction, we would like to point out that the viscoelastic model describing the phase-separation behavior of a dynamically asymmetric mixture could provide a general framework for understanding all these reported features.[77]

V. Conclusions

By means of QENS complemented with DS we have investigated the dynamics of the high-T_g and majority component in the blend 80% PVAc/20% PEO, PVAc. In the glassy state, the methyl group dynamics is not affected by blending. In the region above the glass transition—the main focus of this work—we have arrived at the following conclusions:

•The acceleration in the time scale of PVAc caused by blending is in good agreement with the predictions of the model proposed by Lodge and McLeish.

•The spectral shape and Q dependence of the characteristic times observed by QENS is the same in pure PVAc and in the blend, at least in the temperature region and the overlapping Q range investigated.

•According to the above two points, the influence of blending on the high-T_g component PVAc can be considered as "standard", even being part of a dynamically highly asymmetric mixture.

•In both, PVAc as homopolymer and as blend component, strong deviations from Gaussian behavior are found. The crossover from Gaussian to non-Gaussian regime takes place

at unusually low Q values. This could be attributed to heterogeneities and/or influence of local elementary processes at the origin of the sublinear diffusion in the α-relaxation.

•The emergence of confinement effects in PEO dynamics coincides with the merging of the α- and β-processes in PVAc. Thus, we suggest that the confined PEO motion observed below this temperature is assisted by the local remaining mobility involved in the secondary relaxation of the slow component, while the freezing of the intermolecular correlations of PVAc does not allow accommodation of the large length scale dynamics of PEO.

Acknowledgment. This research project has been supported by the European Commission NoE SoftComp, Contract NMP3-CT-2004-502235. A.A. and J.C. acknowledge support from Projects MAT2004-01017 and 9/UPV00206.215-13568/2001.

References and Notes

(1) Lodge, T. P.; McLeish, T. C. B. *Macromolecules* **2000**, *33*, 5278.
(2) Leroy, E.; Alegría, A.; Colmenero, J. *Macromolecules* **2003**, *36*, 7280.
(3) Hirose, Y.; Urakawa, O.; Adachi, K. *Macromolecules* **2003**, *36*, 3699.
(4) He, Y.; Lutz, T. R.; Ediger, M. D. *J. Chem. Phys.* **2003**, *119*, 9956.
(5) Kant, R.; Kumar, S. K.; Colby, R. H. *Macromolecules* **2003**, *36*, 10087.
(6) Colby, R. H.; Lipson, J. E. G. *Macromolecules* **2005**, *38*, 4919.
(7) Krygier, E.; Lin, G.; Mendes, J.; Mukandela, G.; Azar, D.; Jones, A. A.; Pathak, J. A.; Colby, R. H.; Kumar, S. K.; Floudas, G.; Krishnamoorti, R.; Faust, R. *Macromolecules* **2005**, *38*, 7721.
(8) Hirose, Y.; Adachi, K. *Macromolecules* **2006**, *39*, 1779.
(9) Roland, C. M.; McGrath, K. J.; Casalini, R. *Macromolecules* **2006**, *39*, 3581.
(10) Chung, G.-C.; Kornfield, J. A.; Smith, S. D. *Macromolecules* **1994**, *27*, 5729.
(11) Takegoshi, K.; Hikichi, K *J. Chem. Phys.* **1991**, *94*, 3200.
(12) LeMenestrel, C.; Kenwright, A. M.; Sergot, P.; Laupretre, F.; Monnerie, L. *Macromolecules* **1992**, *25*, 3020.
(13) Cendoya, I.; Alegría, A.; Alberdi, J. M.; Colmenero, J.; Grimm, H.; Richter, D.; Frick, B. *Macromolecules* **1999**, *32*, 4065.
(14) Lorthioir, C.; Alegría, A.; Colmenero, *Phys. Rev. E* **2003**, *68*, 031805.
(15) Colby, R. H. *Polymer* **1989**, *30*, 1275.
(16) Zawada, J. A.; Ylitalo, C. M.; Fuller, G. G.; Colby, R. H; Long, T. E. *Macromolecules* **1992**, *25*, 2896.
(17) Dionísio, M.; Fernandes, A. C.; Mano, J. F.; Correia, N. T.; Sousa, R. C. *Macromolecules* **2000**, *33*, 1002.
(18) Lutz, T. R.; He, Y. Y.; Ediger, M. D.; Cao, H. H.; Lin, G. X.; Jones, A. A. *Macromolecules* **2003**, *36*, 1724.
(19) Sakai, V.; Chen, C.; Maranas, J. K. *Macromolecules* **2004**, *37*, 9975.
(20) Cao, H.; Lin, G.; Jones, A. A. *J. Polym. Sci., Part B: Polym. Phys.* **2005**, *43*, 2433.
(21) Genix, A.-C.; Arbe, A.; Alvarez, F.; Colmenero, J.; Willner, L.; Richter, D. *Phys. Rev. E* **2005**, *72*, 031808.
(22) Farago, B.; Chen, C.; Maranas, J. K.; Kamath, S.; Colby, R. H.; Pasquale, A. J.; Long, T. E. *Phys. Rev. E* **2005**, *72*, 031809.
(23) Sy J. W.; Mijovic, J. *Macromolecules* **2000**, *33*, 933.
(24) Urakawa, O.; Sugihara, T.; Adachi, K. *Polym. Appl. (Jpn.)* **2002**, *51*, 10.
(25) Moreno, A. J.; Colmenero, J. *J. Chem. Phys.*. **2006**, *124*, 184906.
(26) Tyagi, M.; Arbe, A.; Colmenero, J.; Frick, B.; Stewart, J. R. *Macromolecules* **2006**, *39*, 3007.
(27) Lovesey, S. W. *Theory of Neutron Scattering from Condensed Matter*; Clarendon Press: Oxford, U.K., 1984).
(28) Squires, G. L. *Introducction to the Theory of Thermal Neutron Scattering*; Dover Publication Inc.: New York, 1996.
(29) Bee, M. *Quasielastic Neutron Scattering*; Adam Hilger: Bristol, U.K., 1988.
(30) Colmenero, J.; Mukhopadhyay, R.; Alegría, A.; Frick, B. *Phys. Rev. Lett.* **1998**, *80*, 2350.
(31) Moreno, A. J.; Alegría, A.; Colmenero, J.; Frick, B. *Phys. Rev. B* **1999**, *59*, 5983.
(32) Tyagi, M.; Alegría, A.; Colmenero, J. *J. Chem. Phys.* **2005**, *122*, 244909.
(33) Alvarez, F.; Colmenero, J.; Zorn, R.; Willner, L.; Richter, D. *Macromolecules* **2003**, *36*, 238.
(34) Colmenero, J.; Moreno, A.; Alegría, A. *Prog. Polym. Sci.* **2005**, *30*, 1147.
(35) Mukhopadhyay, R.; Alegría, A.; Colmenero, J.; Frick, B. *Macromolecules* **1998**, *31*, 3985.
(36) Moreno, A. J.; Alegría, A.; Colmenero, J. *Phys. Rev. B* **2001**, *63*, R60201.
(37) Zhang, C.; Arrighi, V.; Gagliardi, S.; McEwen, I. J.; Tanchawanich, J.; Telling, M. T. F.; Zanotti, J.-M. *Chem. Phys.* **2006**, *328*, 53.
(38) Götze, W. In *Liquids, Freezing, Glass Transition*; Hansen, J. P., Levesque, D., Zinn-Justin, J., Eds.; North-Holland: Amsterdam, 1991; p 287.
(39) Richter, D.; Monkenbusch, M.; Arbe, A.; Colmenero, J. *Neutron Spin-Echo Investigations on Polymer Dynamics*; Adv. Polym. Sci. 174; Springer-Verlag: Berlin, 2005.
(40) Mukhopadhyay, R.; Alegría, A.; Colmenero, J.; Frick, B. *J. Non-Cryst. Solids* **1998**, *235−237*, 233.
(41) Pérez, Aparicio, R.; Arbe, A.; Colmenero, J.; Schweika, W.; Richter, D.; Fetters, L. J. *Macromolecules* **2006**, *39*, 1060.
(42) Urakawa, O.; Fuse, Y.; Hori, H.; Tran-Cong, Q.; Yano, O. *Polymer* **2001**, *42*, 765.
(43) Arbe, A.; Alegría, A.; Colmenero, J.; Hoffmann, S.; Willner, L.; Richter, D. *Macromolecules* **1999**, *32*, 7572.
(44) Frick, B.; Richter, D. *Science* **1995**, *267*, 1939.
(45) Zorn, R.; Arbe, A.; Colmenero, J.; Frick, B.; Richter, D.; Buchenau, U. *Phys. Rev. E* **1995**, *52*, 781.
(46) Richter, D.; Arbe, A.; Colmenero, J.; Monkenbusch, M.; Farago, B.; Faust, R. *Macromolecules* **1998**, *31*, 1133.
(47) Tyagi, et al. To be published.
(48) Kumar, S. K.; Colby, R. H.; Anastasiadis, S. H.; Fytas, G. *J. Chem. Phys.* **1996**, *105*, 3777.
(49) Kamath, S.; Colby, R. H.; Kumar, S. K.; Karatasos, K.; Floudas, G.; Fytas, G.; Roovers, J. E. L. *J. Chem. Phys.* **1999**, *111*, 6121.
(50) Salaniwal, S.; Kant, R.; Colby, R. H.; Kumar, S. K. *Macromolecules* **2002**, *35*, 9211.
(51) Kamath, S.; Colby, R. H.; Kumar, S. K. *Phys. Rev. E* **2003**, *f67*, 010801(R).
(52) Kamath, S.; Colby, R. H.; Kumar, S. K. *Macromolecules* **2003**, *36*, 8567.
(53) Colmenero, J.; Alegría, A.; Arbe, A.; Frick, B. *Phys. Rev. Lett.* **1992**, *69*, 478.
(54) Colmenero, J.; Arbe, A; Alegría, A. *J. Non-Cryst. Solids* **1994**, *172−174*, 126.
(55) Colmenero, J.; Arbe, A.; Alegría, A.; Monkenbusch, M.; Richter, D. *J. of Phys.: Cond. Matter* **1999**, *11*, A363.
(56) Colmenero, J.; Alvarez, F.; Arbe, A. *Phys. Rev. E* **2002**, *65*, 041804.
(57) Farago, B.; Arbe, A.; Colmenero, J.; Faust, R.; Buchenau, U.; Richter, D. *Phys. Rev. E* **2002**, *65*, 051803.
(58) Arbe, A.; Colmenero, J.; Alvarez, F.; Monkenbusch, M.; Richter, D.; Farago, B.; Frick, B. *Phys. Rev. Lett.* **2002**, *89*, 245701.
(59) Ahumada, O.; Theodorou, D. N.; Triolo, A.; Arrighi, V.; Karatasos, C.; Ryckaert, J. P. *Macromolecules* **2002**, *35*, 7110.
(60) Doxastakis, M.; et al. *J. Chem. Phys.* **2002**, *116*, 4707.
(61) Frick, B.; Dosseh, G.; Cailliaux, A.; Alba-Simionesco, C. *Chem. Phys.* **2003**, *292*, 311.
(62) Arbe, A.; Colmenero, J.; Alvarez, F.; Monkenbusch, M.; Richter, D.; Farago, B.; Frick, B. *Phys. Rev. E* **2003**, *67*, 051802.
(63) Narros, A.; Alvarez, F.; Arbe, A.; Colmenero, J.; Richter, D.; Farago, B. *J. Chem. Phys.* **2004**, *121*, 3282.
(64) Tyagi, M.; Alvarez, F.; Alegría, A.; Colmenero, J.; Frick, B.; Faraone, A. Manuscript in preparation.
(65) Hoffmann, S.; Willner, L.; Richter, D.; Arbe, A.; Colmenero, J.; Farago, B. *Phys. Rev. Lett.* **2000**, *85*, 772.
(66) Chung, G.-C.; Kornfield, J. A.; Smith, S. D. *Macromolecules* **1994**, *27*, 964.
(67) Wu, S. *J. Polym. Sci., Polym. Phys. Ed.* **1989**, *27*, 723.
(68) Zirkel, A.; Richter, D.; Fetters, L. J.; Schneider, D.; Graciano, V.; Hadjichristidis, N. *Macromolecules* **1995**, *28*, 5262.
(69) Urakawa, O.; Ujii, T.; Adachi, K. *J. Non-Cryst. Solids* **2006**, *352*, 5042.
(70) Gómez, D.; Alegría, A.; Arbe, A.; Colmenero, J. *Macromolecules* **2001**, *287*, 503.
(71) Lutz, T. R.; He, Y. Y.; Ediger, M. D.; Pistsikalis, M.; Hadjichistidis, N. *Macromolecules* **2004**, *37*, 6440.
(72) Lutz, T. R.; He, Y. Y.; Ediger, M. D. *Macromolecules* **2005**, *38*, 9826.
(73) Herrera, D.; Zamora, J. C.; Bello, A.; Grimau, M.; Laredo, E.; Müller, A. J.; Lodge, T. P. *Macromolecules* **2005**, **38**, 5109.
(74) Cangialosi, D.; Schwarz, G. A.; Alegría, A.; Colmenero, J. *J. Chem. Phys.*. **2005**, *123*, 144908.
(75) Koizumi, S. *J. Polym. Sci., Part B: Polym. Phys.* **2003**, *42*, 3148.
(76) Doi, M.; Onuki, A. *J. Phys. II* **1992**, *2*, 1631.
(77) Tanaka, H. *J. Phys.: Condens. Matter* **2000**, *12*, R207.

MA070539I